Journal of Pharmaceutical and Biomedical Analysis 149 (2018) 143–150

Contents lists available at ScienceDirect

Journal of Pharmaceutical and Biomedical Analysis

journal homepage: www.elsevier.com/locate/jpba

Characterization of systems with amino-acids and oligosaccharides as modifiers of biopharmaceutical properties of furosemide

Julieta Abraham Miranda [a], Claudia Garnero [a,*], Ariana Zoppi [a], Vanesa Sterren [a], Alejandro P. Ayala [b], Marcela R. Longhi [a]

[a] Unidad de Investigación y Desarrollo en Tecnología Farmacéutica (UNITEFA), CONICET and Departamento de Ciencias Farmacéuticas, Facultad de Ciencias Químicas, Universidad Nacional de Córdoba, Ciudad Universitaria, 5000 Córdoba, Argentina
[b] Department of Physics, Federal University of Ceará, Fortaleza, Ceará, Brazil

ARTICLE INFO

Article history:
Received 15 August 2017
Received in revised form 26 October 2017
Accepted 28 October 2017
Available online 2 November 2017

Keywords:
Furosemide
Amino-acids
Arginine
β-cyclodextrin
Maltodextrin
Solubility

ABSTRACT

Furosemide is the most commonly prescribed diuretic drug in spite of its suboptimal biopharmaceutical properties. In this work, the addition of different amino-acids was studied with the aim of selecting an enhancer of the furosemide solubility. The best results were obtained with arginine. Also, binary (furosemide:arginine) and ternary (furosemide:arginine:β-cyclodextrin and furosemide:arginine:maltodextrin) systems were prepared by the kneading method and they were compared with their corresponding physical mixtures. These new systems were characterized by Fourier transform infrared and Raman spectroscopy, X-ray powder diffractometry, scanning electron microscopy, thermogravimetric analysis, and differential scanning calorimetry. In addition, dissolution studies were performed in simulated gastric fluid. The best results in relation to improving biopharmaceutical properties were obtained with a binary combination of furosemide and arginine, demonstrating that this system could result in a suitable candidate for the development of a promising pharmaceutical formulation of the drug.

1. Introduction

Oral administration of drugs is the most extensively used route due to its improved convenience and patient compliance. However, there is a variety of challenges associated with this route such as incomplete absorption of drugs, short residence time of formulations and degradation in the gastrointestinal tract, hepatic metabolism [1,2] added to the low bioavailability of most drugs due to their low solubility and permeability [3]. Numerous methodologies were developed to improve the solubility of drugs such as complex or salt formation [4,5], cocrystallization or coamorphization [6,7], molecular dispersions in polymer carriers [8,9], size reduction or micronization [10], and polymorph selection [11]. Recently, amino-acids (AA) have been studied as strategies to enhance the biopharmaceutical properties of drugs such as solubility, dissolution rate, permeability, and/or stability [12–14]. For example, arginine (ARG), cysteine (CYS), glycine (GLY), and leucine (LEU) were combined with chloramphenicol (CP) by the freeze-drying method to enhance the dissolution rate and decrease the oxidative stress produced by this drug, with CP:LEU showing the best results [15]. In addition, ARG demonstrated to have positive effects on different properties of drugs. In particular, in the co-amorphous system between ARG and indomethacin, the dissolution behaviour of the drug was noticeably improved [16]. Furthermore, it was demonstrated that ARG can be used as a potential absorption enhancer because it can accelerate the development of oral delivery systems for insulin without any toxic effects such as membrane disruption and tight junction opening [17]. Other recent study has revealed that the physicochemical properties of cefexime were greatly improved by the synergistic effect of ARG and cyclodextrins (CD) on the formation of inclusion compounds compared with those of the pure drug [18]. In addition, ternary complexation involving salt formation with organic or inorganic cations was successfully applied to improve the β-CD solubilizing capacity towards acidic drugs [19,20]. In this regard, the use of basic AAs as counter-ions for ternary complex formation with β-CD and acidic drugs proved to be particularly effective [21–24].

Furosemide (FUR) is a loop diuretic drug widely used for the treatment of hypertension and edema. However, its bioavailability

* Corresponding author.
E-mail addresses: jmiranda@fcq.unc.edu.ar (J.A. Miranda), garneroc@fcq.unc.edu.ar (C. Garnero), ariana@fcq.unc.edu.ar (A. Zoppi), vsterren@fcq.unc.edu.ar (V. Sterren), ayala@fisica.ufc.br (A.P. Ayala), mrlcor@fcq.unc.edu.ar (M.R. Longhi).

https://doi.org/10.1016/j.jpba.2017.10.038
0731-7085/

is highly variable when it is orally administered since FUR has a low aqueous solubility and a poor permeability (class IV in the Biopharmaceutics Classification System (BCS) [25]). It also has a tendency to undergo site-specific absorption in the stomach and upper small intestine [26,27].

Therefore, considering the strategies mentioned above, the aim of this study was to select an AA that improves the solubility and/or dissolution rate of the drug and to study the effect of different oligosaccharides (O) forming the multicomponent systems FUR:AA:O on these properties. It was interesting to investigate the possible effect of AA on the enhancement of the complexation and solubilization capabilities of β-CD for FUR. This would allow a more efficient and safe use of β-CD in the development of new and more effective delivery systems of this sulfamide drug based on such ternary systems.

Different AAs were introduced as a promising alternative to enhance the biopharmaceutical properties of FUR. The selected AAs are approved to be used in pharmaceutical applications and some of them are good salt formers due to their ionizable properties and their water solubility [28]. Therefore, the solubility of FUR in the presence of LEU, isoleucine (ILE), valine (VAL), ARG, aspartic acid (ASP), glutamic acid (GLU), histidine (HIS), serine (SER), PRO, lysine (LYS), and GLY was studied. Then, β-CD or maltodextrin (MD) was added as a third component to the binary system FUR:AA with the best properties because they have the capacity to enhance the solubility and/or stability of drugs and food [29–31].

In addition, dissolution studies were performed for the binary and ternary systems of FUR using the kneading method and physical mixture. Also, the systems were characterized by Fourier transform infrared and Raman spectroscopy, X-ray powder diffractometry, scanning electron microscopy, thermogravimetric analysis, and differential scanning calorimetry.

2. Materials and methods

2.1. Chemicals and reagents

Furosemide was provided by Parafarm (Argentina). L-Leucine, L-Arginine, and L-Serine were given by Sigma-Aldrich, USA. L-Isoleucine, L-Valine, Proline, L-Lysine Monohydrochloride, and Glycine were purchased from Todo Droga. L-Aspartic Acid and L (+) Glutamic Acid were provided by Anedra and L-Histidine by Sigma-Aldrich, Japan. β-cyclodextrin (MW = 1135) was kindly supplied by Ferromet agent of Roquette (France) and Maltodextrin (DE17) was obtained from Todo Droga (Argentina). All other chemicals were of analytical grade. A Millipore Milli Q Water Purification System (Millipore, Bedford, MA, USA) generated the water used in these studies.

2.2. Solubility studies

Solubility analyses were carried out according to the method reported by Higuchi & Connors [32]. To determine the AA with the best effect on solubility, an excess of FUR (50 mg) and a 10 mM aqueous solution of different AAs (LEU, ILE, VAL, ARG, ASP, GLU, HIS, SER, PRO, LYS, GLY) were placed in stoppered glass tubes at 37 °C. The tubes were placed in an orbital incubator shaker at 180 rpm for 72 h. After equilibrium was reached, the suspensions were filtered through a 0.45 mm membrane filter (Millipore), and the filtrate was appropriately diluted for quantitative analysis of FUR. Each experiment was repeated at least three times and the results reported were the mean values. The quantitative determinations of FUR were performed spectrophotometrically (Shimadzu UV-Mini 1240 spectrophotometer) at 274 nm.

Additionally, the effect of binary and ternary systems on solubility was studied in water, simulated gastric fluid (SGF) and buffer solution of pH 7.4 using ARG, βCD, and MD as ligands. An excess of FUR (50 mg) and different amounts of ARG (3–20 mM), ARG:βCD (3–20 mM:4.3 mM), ARG:βCD (3 mM:2–15 mM), ARG:MD (3–20 mM:4.3 mM), and ARG:MD (3 mM:2–10 mM) were placed in stoppered glass tubes at 37 °C, and then these tubes underwent the process previously described. The stability of the drug was also determined in water, SGF and buffer solution of pH 7.4 at 37 °C and no drug degradation was found after 72 h of incubation.

2.3. Solid sample preparations

Different solid-state systems of FUR were prepared in 1:1 and 1:2 molar relations for binary systems with ARG and in a 1:1:1 molar relation for the ternary systems with ARG and β-CD or MD as follows:

2.3.1. Kneading method (KN)

The binary (B) FUR:ARG (*KN*-$B_{1:1}$ and *KN*-$B_{1:2}$) and the ternary (T) FUR:ARG:β-CD (*KN*-T_{CD}) and FUR:ARG:MD (*KN*-T_{MD}) systems were prepared by accurately weighing appropriate amounts of FUR, ARG and β-CD or MD and then transferred to a mortar. Water was added to the powder mix in a relation of 0.25 μl per mg of solid and the resultant slurry was kneaded for about 60 min. The resultant powder was dried and protected from light under vacuum at room temperature for 48 h. Also, FUR (*KN*$_{FUR}$) and ARG (*KN*$_{ARG}$) were subjected to the KN.

2.3.2. Physical mixture (PM)

The physical mixtures of the binary FUR:ARG (*PM*-$B_{1:1}$ and *PM*-$B_{1:2}$) and the ternary FUR:ARG:β-CD (*PM*-T_{CD}) and FUR:ARG:MD (*PM*-T_{MD}) were prepared by simply blending the corresponding components in a mortar for about 5 min.

2.4. Solid state characterization

2.4.1. X-ray powder diffraction

X-ray powder diffraction (XRPD) was used to investigate the crystalline structure of the systems. The material was ground and mounted on a glass sample holder and the Powder x-ray diffraction patterns were recorded using a D8 Advanced system (Bruker AXS) equipped with a theta/theta goniometer configured in the Bragg Brentano geometry with a fixed specimen holder, using a Cu Kα (0.15419 nm) radiation source and a LynxEye detector. The voltage and electric current applied were 40 kV and 40 mA, respectively. The slit width used for the beam incident on the sample was 0.6 mm. Samples were scanned between (2θ) 5–40° in a step-scan mode (0.01 step size and 5 seg).

2.4.2. FT-IR spectroscopy

The FT-IR spectra of FUR, ARG, β-CD, MD, and all the KN and PM systems were recorded on a Nicolet Avatar 360 FT-IR spectrometer, with the potassium bromide disks being prepared by compressing the powders. The spectra of the samples were obtained and processed using the EZ 153 OMNIC E.S.P v.5.1 software.

2.4.3. Raman spectroscopy

The Raman spectra of the raw materials and the systems were recorded on a LabRAM HR (Horiba) spectrometer equipped with a liquid N_2-cooled CCD detector with a near infrared laser (785 nm) for excitation.

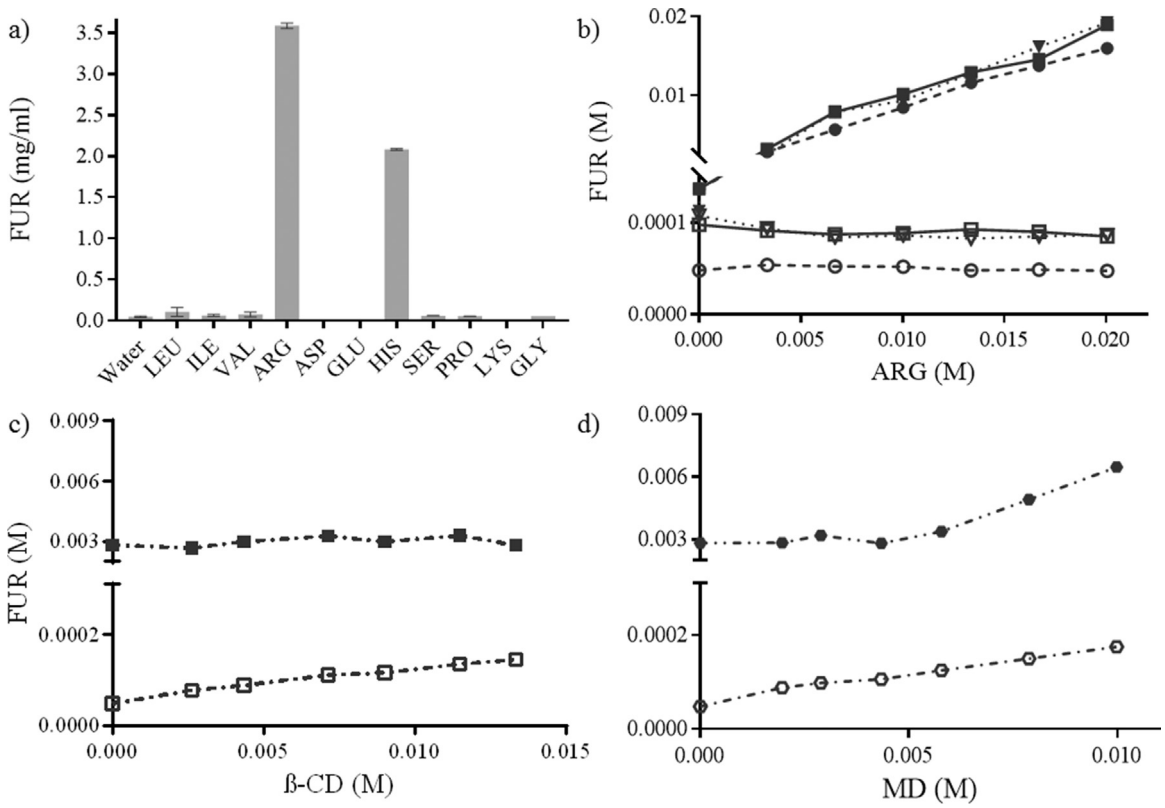

Fig. 1. Effect of: a) Different AAs, b) ARG (●), ARG:β-CD (■), and ARG:MD (▼) in water and ARG (○), ARG:β-CD (□), and ARG:MD (▽) in FGS, c) ARG:β-CD in water (■) and FGS (□) and d) ARG:MD in water (●) and FGS (○) on the solubility of FUR.

2.4.4. SEM

The microscopic morphological structures of the raw materials and the solid samples were investigated and photographed using a Carl Zeiss Σigma scanning electron microscope in the Laboratorio de Microscopía y Análisis por Rayos X (LAMARX) of the National University of Córdoba. The samples were fixed on a brass stub using double-sided aluminium tape. To improve the conductivity, they were gold-coated under vacuum employing a sputter coater Quorum 150. The magnification selected was sufficient to appreciate in detail the general morphology of the samples under study.

2.4.5. Thermal analysis (DSC and TGA)

Thermogravimetric analysis (TGA) and Differential Scanning Calorimetric (DSC) curves were obtained simultaneously using a STA 449 Jupiter system (Netzsch, Germany). Measurements were obtained starting at room temperature up to 450 °C with a heating rate of 10 K min^{-1} using a sealed aluminium crucible with pierced lids containing 5 mg of sample. The sensors and the crucibles were under a constant flow of nitrogen (70 ml/min) during the experiment.

2.5. Dissolution study

The dissolution tests were carried out at 37° C using the USP XXX paddle apparatus (Hanson SR II 6 Flask Dissolution Test Station, Hanson Research Corporation, Chatsworth, CA, USA) with three replicates. The dissolution medium was SGF without enzymes prepared according to USP XXX. Testing was conducted on samples of FUR and also on the systems *KN*-$B_{1:1}$, *KN*-$B_{1:2}$, *KN*-T_{CD}, *KN*-T_{MD}, *PM*-$B_{1:1}$, *PM*-$B_{1:2}$, *PM*-$T_{CD,}$ and *PM*-T_{MD}. Suitable quantities of each powder containing 40 mg of drug were immersed in 900 ml of the dissolution medium at 37 (±0.5) °C and agitated at 50 (±5) rpm. The samples were collected at prearranged time intervals with replacement before being filtered and appropriately diluted with SGF. The amount of the dissolved drug in the samples was analyzed spectrophotometrically at 274 nm. The cumulative percentages of the drug released from the powder, the difference factor (*f1*) and the similarity factor (*f2*) [33] were calculated as:

$$f1 = \frac{\sum_{t-1}^{R} |Rt - Tt|}{\sum Rt} \times 100 \quad (1)$$

$$f2 = 50 \log\{\left[1 + \frac{1}{n}\sum_{t=1}^{n}(R_t - T_t)^2\right]^{-0,5} 100\} \quad (2)$$

where n is the number of sampling points and R_t and T_t are the percentages dissolved of the reference and the test product, respectively, at each time point t. This model is used to estimate the closeness between in vitro dissolution profiles [34].

3. Results and discussion

3.1. Solubility studies

The effect of several AAs on the solubility of FUR at 37.0 ± 0.1 °C was investigated. These AAs with different acid-base characteristics are ASP, GLU, ARG, HIS, LYS, LEU, ILE, VAL, SER, PRO, and GLY. The results obtained (Fig. 1a) demonstrated that ARG was the best candidate for these studies because it increased 77 times the solubility of FUR in water, while HIS increased it 44 times. LEU, ILE, and VAL doubled the solubility of FUR, but SER, PRO, and GLY did not increase it. ASP, GLU, and LYS even reduced it. From these results, ARG was selected as the optimum ligand to study its effect on the solubility of FUR. In addition, the effect of the ternary systems ARG:β-CD and

Table 1
Summary of solubility studies at 37.0 ± 0.1 °C.

System	Solvent	S_o (mg/mL)	S_{max} (mg/mL)	(S_{max}/S_0)	K_C (M^{-1})	Isotherm
FUR:ARG(3–20 mM)	Water	0.047[1]	5.3	113	13875	A_L
FUR:ARG(3–20 mM):β-CD(4.3 mM)		0.047[2]	6.3	134	13223	A_L
FUR:ARG(3–20 mM):MD(4.3 mM)		0.049[2]	6.3	129	240000	A_L
FUR:ARG(3 mM):β-CD(2–15 mM)		0.93[2]	1.1	1	–	B_I
FUR:ARG(3 mM):MD(2–10 mM)		0.93[2]	2.1	2.3	–	A_P
FUR:ARG(3–20 mM)	SGF	0.016[1]	0.017	1	–	B_I
FUR:ARG(3–20 mM):β-CD(4.3 mM)		0.032[2]	0.031	1	–	B_I
FUR:ARG(3–20 mM):MD(4.3 mM)		0.035[2]	0.031	1	–	B_I
FUR:ARG(3 mM):β-CD(2–15 mM)		0.017[2]	0.052	3	117	A_L
FUR:ARG(3 mM):MD(2–10 mM)		0.017[2]	0.058	3.4	194	A_L

So: [1]Solubility of free FUR, [2]Solubility of FUR in presence of the ligand at constant concentration; S_{max}: maximum solubility of the system.

ARG:MD on the solubility of FUR was investigated in water, SGF and buffer solution of pH 7.4. Fig. 1b–d shows the phase solubility diagrams obtained, in water and SGF, by plotting the changes in FUR solubility as a function of the concentration of the ligands. The diagrams were classified according to Higuchi and Connors [32] (Table 1). The results obtained in buffer solution of pH 7.4 are shown in TableS1 (Supporting Information).

The profiles obtained in water showed a linear increase in the solubility of the drug as the concentration of ARG increased. The solubility of FUR in water was 0.047 mg/ml, while in ARG solution the solubility of the drug was from 0.93 mg/ml in a 3 mM ARG solution to 5.3 mg/ml in a 20 mM ARG solution (Fig. 1b). In the ternary systems ARG(3–20 mM):β-CD(4.3 mM) and ARG(3–20 mM):MD(4.3 mM), the increase in the solubility of FUR was slightly higher than in the binary FUR:ARG system (Table 1). On the other hand, in SGF the binary and ternary systems did not modify the solubility of FUR with increasing concentrations of ARG; however, in the ternary systems an increment with respect to the solubility of free FUR was observed due to the addition of increasing amounts of β-CD and MD (Fig. 1b).

In addition, the amount of ARG was fixed at 3 mM, while the concentration of the oligosaccharides was increased to evaluate their effect. The system ARG(3 mM):β-CD(2–15 mM) in aqueous solution did not increase the solubility of FUR, while ARG(3 mM):MD(2–10 mM) did not increase the solubility of the drug up to 4 mM of MD and then showed a linear increase. In SGF, both ARG(3 mM):β-CD(2–15 mM) and ARG(3 mM):MD(2–10 mM)) systems showed a linear increase in the solubility of the drug (Fig. 1c and d). Also, the apparent stability constant (K_C) values (Table 1) were estimated from the slope of the initial linear portion of the diagrams according to the following equation:

$$Kc = \frac{slope}{So\,(1 - slope)} \quad (3)$$

From the K_C values and the analysis of the effects of pH, it can be observed that ionization affected the interaction of FUR with the ligands. The results revealed that the ionized FUR had a greater affinity for ARG, while the unionized FUR (at pH 1.2), with a more lipophilic form, had a better affinity for β-CD and MD than the ionized specie.

3.2. Solid state characterization

3.2.1. XRPD

The XRPD patterns of the raw materials and the systems are shown in Fig. 2 and Fig.S1 (Supporting Information). The diffraction patterns of FUR, ARG, and β-CD exhibited characteristic peaks that were consistent with their crystalline nature, while MD showed an amorphous structure. These result are in good agreement with those previously reported [35,36]. The diffractograms of *KN*-$B_{1:1}$ and *KN*-$B_{1:2}$ showed a decrease in the degree of crystallinity. From the in-depth analysis of these diffractograms, the most intense peaks of FUR were observed behind an amorphous phase in *KN*-$B_{1:1}$, but no peaks of ARG were found. However, in *KN*-$B_{1:2}$, the amorphous phase was present, as well as the most intense peaks of FUR and some peaks of ARG. This could be due to the different amounts of ARG in the systems. Then, FUR and ARG in free form were subjected to the same kneading procedure. The patterns showed that FUR and ARG maintained their crystalline structure after the treatment (Fig. S1). Thus, in *KN*-$B_{1:1}$ and *KN*-$B_{1:2}$, the ARG structure was mostly amorphized when it was kneaded in the presence of the drug, while FUR maintained its crystalline structure. This decrease in the crystallinity of the system could lead to a decrease in the stability of the drug because, as it is known, the amorphous solids tend to crystallize. From this analysis, the addition of β-CD or MD could be a strategy to stabilize the system. The pattern of *KN*-T_{MD} showed a decrease in the degree of crystallinity, but it was expected because MD is an amorphous solid. However, *KN*-T_{CD} maintained the crystallinity of all the components. Therefore, *KN*-T_{CD} and *KN*-T_{MD} could be interesting strategies to stabilize the amorphous system of FUR:ARG. One of them helped maintain all solids in a crystalline state and the other one, which is a solid, allowed the system to remain amorphous and stable. On the other hand, the diffractograms of *PM*-$B_{1:1}$, *PM*-$B_{1:2}$, *PM*-T_{CD}, and *PM*-T_{MD} showed the superimposition of the characteristic peaks of all the component patterns although at lower intensity due to the dilution of the raw materials. These results indicated absence of interaction between the components.

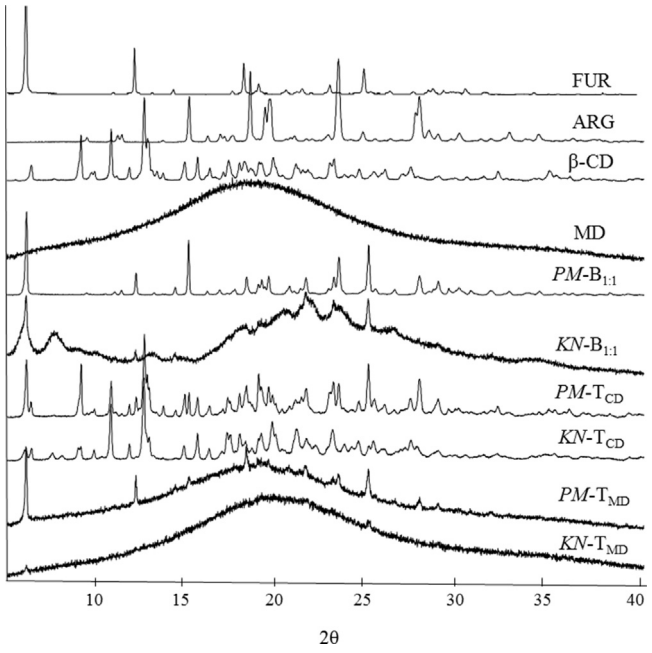

Fig. 2. XRPD patterns of FUR, ARG, β-CD, MD and the systems.

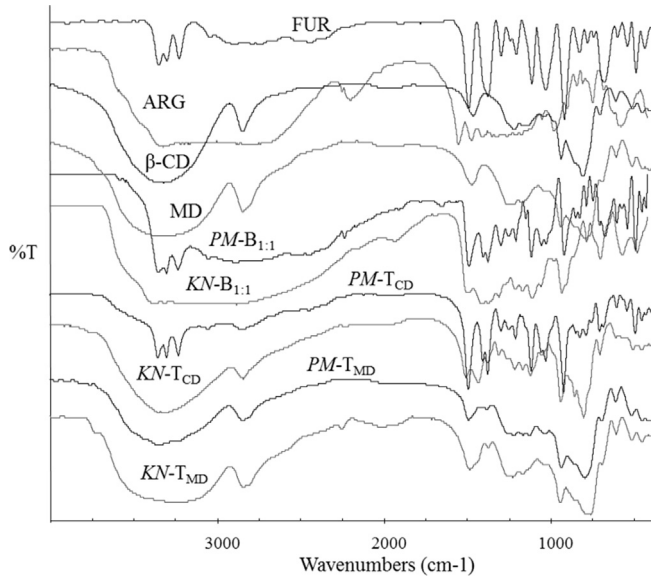

Fig. 3. FT-IRspectra of FUR, ARG, β-CD, MD, and the binary and ternary systems.

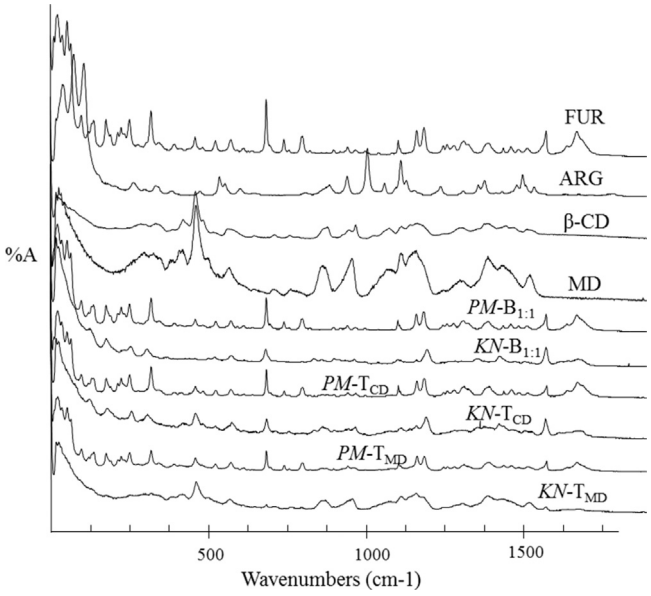

Fig. 4. Raman spectra of the raw materials and the systems.

3.2.2. FT-IR spectroscopy

The FT-IR spectra of the raw materials and the systems are presented in Fig. 3 and Fig. S2. The FT-IR spectrum of FUR was characterized by bands at 3397 and 3285 cm^{-1} (sulfonamide NH stretch), 3353 cm^{-1} (secondary amine NH stretch), 1324 cm^{-1} and 1141 cm^{-1} (S=O stretch), and 1673 cm^{-1} (C=O stretch). The observed spectrum agrees with those previously reported [35]. The FT-IR spectrum of the binary system *KN*-$B_{1:1}$ showed the appearance of a new band at 1611 cm^{-1} which could correspond to the COO^- group and the shift of the bands corresponding to S=O stretch from 1324 cm^{-1} and 1141 cm^{-1} to 1311 cm^{-1} and 1147 cm^{-1}, respectively. However, the spectrum of the system *KN*-$B_{1:2}$ did not show differences compared with that of *KN*-$B_{1:1}$ (Fig. S2). On the other hand, the spectra of the ternary systems *KN*-T_{CD} and *KN*-T_{MD} showed the shift of one of the bands corresponding to S=O stretch from 1141 cm^{-1} to 1155 cm^{-1} and 1160 cm^{-1}, respectively. The FUR signals in the region of 3200 cm^{-1} to 3600 cm^{-1} overlapped with those of the OH^- group of the oligosaccharides. In addition, *KN*-T_{CD} showed the presence of a band at 1615 cm^{-1}, which was present in the binary systems (*KN*-$B_{1:1}$ and *KN*-$B_{1:2}$), and the appearance of a new band at 1263 cm^{-1}. Nevertheless, the spectra of PMs corresponded simply to the superposition of the FT-IR spectra of the components. The results of the FT-IR studies suggest that ARG can form a salt with FUR in the KN binary systems, which is in agreement with the report of Jensen et al. [37] on the obtainment of a FUR:ARG salt by ball milling. On the other hand, this FUR:ARG salt interacted with β-CD in the ternary systems. Although a band was not observed at 1611 cm^{-1} in the MD ternary system, we cannot ensure that the salt was not formed.

3.2.3. Raman spectroscopy

The Raman spectra are shown in Fig. 4 and Fig. S3. FUR was characterized by bands at 3271 cm^{-1} (sulfonamide NH stretch), 3348 cm^{-1} (secondary amine NH stretch), 1338 cm^{-1}, and 1147 cm^{-1} (S=O stretch). The spectra of *KN*-$B_{1:1}$ and *KN*-$B_{1:2}$ showed small shifts, the disappearance of bands from FUR and ARG, the appearance of a new band at 1302 cm^{-1}, and the shift of the bands corresponding to S=O stretch from 1338 cm^{-1} and 1147 cm^{-1} to 1369 cm^{-1} and 1156 cm^{-1}, respectively (Fig. S3). The *KN*-T_{CD} system exhibited modifications in the spectral regions of 350–550 cm^{-1} and 1200–1350 cm^{-1}, the disappearance of a band at 1010 cm^{-1}, and a shift of the bands corresponding to S=O stretch from 1338 cm^{-1} and 1147 cm^{-1} to 1312 cm^{-1} and 1154 cm^{-1}, respectively. Although peaks corresponding to MD could be observed for KN-T_{MD}, several bands of the binary system were maintained between 1500 and 1650 cm^{-1} and 650–800 cm^{-1}. One band corresponding to *KN*-$B_{1:1}$ and *KN*-$B_{1:2}$ was also observed at 280 cm^{-1}. However, it was not possible to observe the band corresponding to the COO— group which was present in the FT-IRspectra. On the other hand, PMs simply showed the superposition of the spectra of the components. These results are consistent with those obtained by FT-IR spectroscopy.

3.2.4. SEM

Supporting morphological evidence of the interaction between FUR and ARG, β-CD or MD obtained from SEM is presented in Fig. 5. It shows the distinct morphological differences between the samples. As stated in previous reports, FUR showed hexagonal tubular crystals, β-CD exhibited an irregular shape with cracks and smaller particles on the surface of large particles, and MD displayed spherical particles with adherence to smaller spherical entities [35,36]. The microphotograph of ARG showed large, flat and rough structures. The SEM images of the KN systems showed particles with changes in their morphology and size compared with the components. In these systems, it could be observed that the original morphology of the components disappeared, suggesting interaction of the drug with the ligands in the solid state. The images of *KN*-$B_{1:1}$, *KN*-$B_{1:2}$, *KN*-$T_{CD,}$ and *KN*-T_{MD} showed compact structures with irregular size and shape and adherence of particles of different sizes. The system containing β-CD exhibited rough structures, while the one containing MD showed smooth structures. The drastic changes in the particle shape and size revealed the presence of new solid phases in the systems of KNs and evidence of interaction. On the other hand, the original morphology of all the components could be observed in the images of PMs. The results obtained by SEM were well correlated with those obtained by XRPD.

3.2.5. DSC and TGA

The DSC and TGA profiles of the raw materials and the systems are shown in Fig. 6 and Fig. S4. The DSC profile of FUR is in agreement with those previously reported [38–41]. It exhibited a weak endotherm at 136.1 °C without mass loss in the TGA curve over the range 130–140 °C, indicating a likely polymorphic phase transition (form IV melts and immediately crystallizes to form I), a very

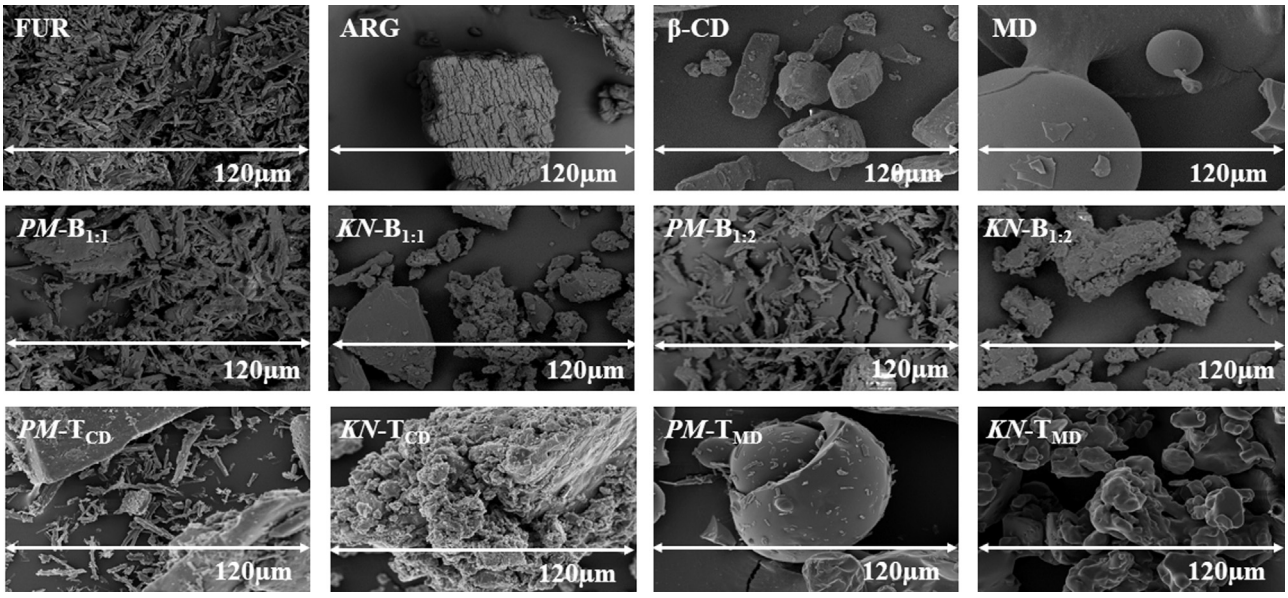

Fig. 5. Microphotography of the raw materials and the binary and ternary systems.

small melting endotherm at 219.9 °C followed by a sharp exotherm at 223.6 °C associated with the decomposition of the drug, and two endotherms at 271 and 281.9 °C attributed to the decomposition phenomena of the material. The β-CD and MD profiles showed broad endotherms between 50 and 175 °C associated with the dehydration phenomena. At above 300 °C, the profiles showed weight loss (registered by TGA), which was assigned to the degradation phenomena. The DSC profile of ARG is in line with previous report [23]. It showed three endotherms. One of them was observed at 102 °C with mass loss in the TGA curve over the range 55–115 °C, indicating that in a small portion of the sample, ARG was present as a dehydrated form. The second endotherm appeared at 222 °C, which corresponded to the melting of anhydrous ARG accompanied by decomposition. The last one at 239 °C was attributed to the total decomposition. The DCS curve of the KNs showed the complete disappearance of the FUR thermal events, confirming the molecular interaction of the drug with the ligands. However, the PMs showed the characteristic events of the individual components, suggesting that the interaction between the KNs and the PMs was different. The TGA curves for *KN*-$B_{1:1}$, *PM*-$B_{1:1}$, *KN*-$B_{1:2}$, *PM*-$B_{1:2}$, *KN*-T_{CD}, *PM*-T_{CD}, *KN*-T_{MD}, and *PM*-T_{MD} revealed a dehydration process with a mass loss of 5.3%, 8.1%, 6.3%, 8.8%, 12.8%, 8.6%, 9.1, and 5.9%, respectively.

3.3. Dissolution study

Dissolution experiments were carried out to evaluate the effect of the ligands on the dissolution of FUR. The dissolution profiles of FUR and of the binary and ternary systems are shown in Fig. 7. In addition, to compare the dissolution profiles of the systems with that of free FUR, the difference factor (*f1*) and the similarity factor (*f2*) were calculated (Table 2). All the examined systems exhibited faster dissolution rates than the drug alone. After 120 min, only a 12% of the total free FUR was in solution, while in the eight systems the percentage of FUR dissolved was always higher (Table 2).

In general, *f1* value lower than 15 (0–15) and *f2* value higher than 50 (50–100) indicated the similarity of the two dissolution profiles. In all cases, *f1* and *f2* values were higher than 15 and lower than 50, respectively, indicating that the dissolution profiles of all systems exhibited clear differences in dissolution rate compared with those of free FUR. Moreover, the KN systems showed improved

Table 2
Percentage of FUR dissolved at different times, *f1* and *f2* values.

	% FUR dissolved (5 min)	% FUR dissolved (120 min)	*f1*	*f2*
FUR	Not quantifiable	12	–	–
PM-$B_{1:1}$	4	25	70	46
KN-$B_{1:1}$	10	35	82	31
PM-$B_{1:2}$	11	31	80	34
KN-$B_{1:2}$	24	69	92	12
PM-T_{CD}	4	25	69	46
KN-T_{CD}	6	30	75	39
PM-T_{MD}	7	29	78	36
KN-T_{MD}	11	34	82	31

dissolution rates compared with their respective PM. Additionally, the dissolution parameters (dissolution rate and percentage of drug dissolved) of the KN-$B_{1:2}$ system were almost 2 times higher than the corresponding values obtained with all the other products (Fig. 7). Therefore, on the basis of these results, it is reasonable to hypothesize a specific role of ARG in the formation of the systems in solid state as a result of the interaction of a basic AA with the acidic drug (through electrostatic interactions and salt formation). In fact, FUR, while interacting with ARG that acts as a counter-ion, can form a more hydrophilic structure and thus enhance its wettability and dissolution. This effect is maximized when 2 molecules of AA are associated with the drug. In addition, this binary system can be seen as an amphiphilic structure that interacts with the hydrophobic part of both oligosaccharides through complex formation, thus decreasing crystallinity and favouring the solubility of FUR.

4. Conclusions

In the present investigation, the study of the effect of several AAs on the solubility of FUR allowed selecting ARG as the best candidate for being an enhancer of the drug properties. Then, two binary systems combining FUR with ARG in different amounts and two ternary systems with β-CD or MD as third components were developed and characterized. The solid-state characterization of the systems by FT-IR, Raman, XRPD, SEM, and DSC/TG showed that FUR and ARG interact with each other through ionic bonds forming a salt that interacts with β-CD or MD to form ternary systems. In the dissolution assays, the system KN-$B_{1:2}$ showed significantly

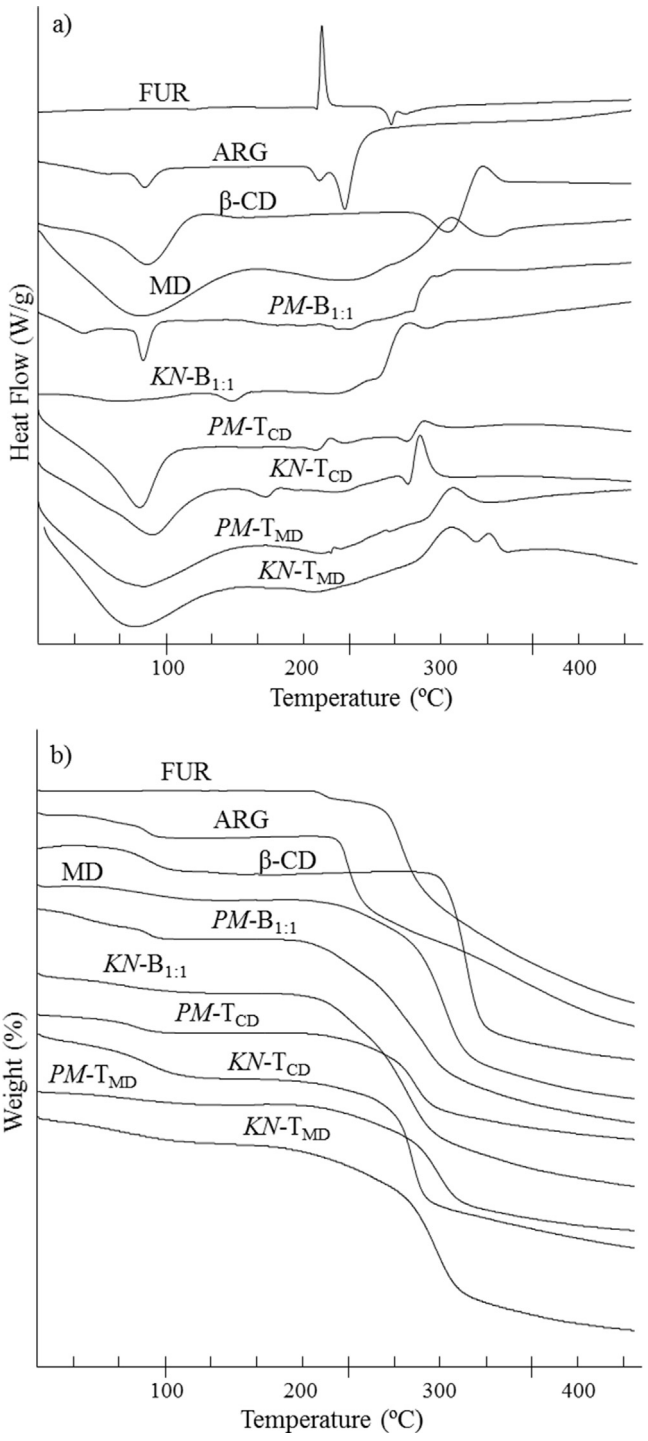

Fig. 6. DSC (a) and TG (b) of the raw materials and the binary and ternary systems.

better properties because it allowed dissolution of about 70% of the drug within 120 min, while the pure drug dissolved 12% and all the other systems dissolved about 30% of the drug. Considering that the binary system FUR:ARG obtained by KN was amorphous and probably unstable, the presence of oligosaccharides could be an interesting alternative to stabilize their solid state and to maintain the improvement of solubility. Therefore, these systems are appropriate candidates for further studies oriented towards the development of a promising pharmaceutical formulation of FUR for oral delivery.

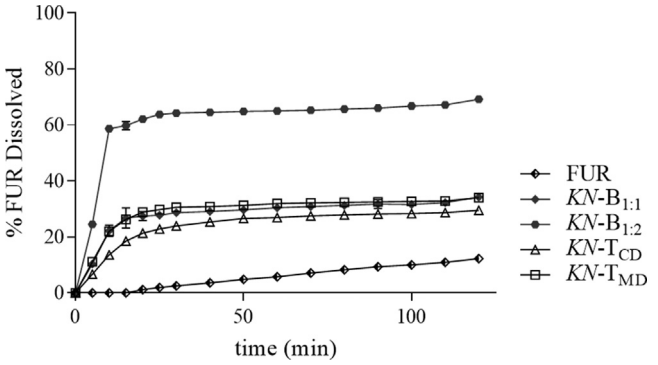

Fig. 7. Dissolution profiles of suitable quantities of each powder containing 40 mg of FUR in SGF at 37 (±0.5) °C.

Supporting information

This material show the results of solubility studies obtained in buffer solution of pH 7.4, and the spectral and thermal behaviors of binary systems 1:1 and 1:2 constituted by furosemide (FUR) and arginine (ARG). The systems were characterized by XRPD (Fig. S1), FTIR (Fig. S2) and Raman (Fig. S3) spectroscopy and thermal analysis (Fig. S4). Also, the XRPD patterns of FUR and ARG submitted to de kneading method are show.

Acknowledgments

The authors wish to acknowledge the assistance of the Consejo Nacional de Investigaciones Científicas y Técnicas (CONICET) and the Universidad Nacional de Córdoba, both of which provided support and facilities for this investigation. Moreover, the project MinCyT-CONICET-CAPES is gratefully acknowledged. The researchers also thank the Secretaría de Ciencia y Técnica de la Universidad Nacional de Córdoba (SECyT-UNC) and Fondo para la Investigación Científica y Tecnológica (FONCYT) for financial support.

Appendix A. Supplementary data

Supplementary data associated with this article can be found, in the online version, at https://doi.org/10.1016/j.jpba.2017.10.038.

References

[1] B.F. Choonara, Y.E. Choonara, P. Kumar, D. Bijukumar, L.C. du Toit, V. Pillay, A review of advanced oral drug delivery technologies facilitating the protection and absorption of protein and peptide molecules, Biotechnol. Adv. 32 (2014) 1269–1282, http://dx.doi.org/10.1016/j.biotechadv.2014.07.006.
[2] A. Sosnik, Alginate particles as platform for drug delivery by the oral route: state-of-the-Art, ISRN Pharmaceutics (2014), http://dx.doi.org/10.1155/2014/926157.
[3] D. Sharma, S. Joshi, Solubility enhancement strategies for poorly water soluble drugs in solid dispersion: a review, Asian J. Pharm. 1 (2007) http://www.asiapharmaceutics.info/pdf/2rew_solibilty.pdf.
[4] S.K. Nechipadappu, D.R. Trivedi, Pharmaceutical salts of ethionamide with GRAS counter ion donors to enhance the solubility, Eur. J. Pharm. Sci. 96 (2017) 578–589, http://dx.doi.org/10.1016/j.ejps.2016.10.035.
[5] S.S. Jambhekar, P. Breen, Cyclodextrins in pharmaceutical formulations I: structure and physicochemical properties, formation of complexes, and types of complex, Drug Discov. Today 21 (2016) 356–362, http://dx.doi.org/10.1016/j.drudis.2015.11.017.
[6] S.G. Kuminek, G. Rodriguez-Hornedo, N. Siedler, S. Rocha, H.V.A. Cuffini, S.L. Cardoso, How cocrystals of weakly basic drugs and acidic coformers might modulate solubility and stability, Chem. Commun. 52 (2016) 5832–5835, http://dx.doi.org/10.1039/C6CC00898D.
[7] K. Löbmann, R. Laitinen, C. Strachan, T. Rades, H. Grohganz, Amino acids as co-amorphous stabilizers for poorly water-soluble drugs – part 2: molecular interactions, Eur. J. Pharm. Biopharm. 85 (2013) 882–888, http://dx.doi.org/10.1016/j.ejpb.2013.03.026.

[8] W. Xu, P. Ling, T. Zhang, Polymeric micelles, a promising drug delivery system to enhance bioavailability of poorly water-soluble drugs, J. Drug Deliv. (2013) 2013, http://dx.doi.org/10.1155/2013/340315.
[9] S. Caban, E. Aytekin, A. Sahin, Y. Capan, Nanosystems for drug delivery, OA Drug Des. Deliv. 2 (2014) 1–7.
[10] R. Campardelli, E. Oleandro, M. Scognamiglio, G. Della Porta, E. Reverchon, Palmitoylethanolamide sub-micronization using fast precipitation followed by supercritical fluids extraction, Powder Technol. 305 (2017) 217–225, http://dx.doi.org/10.1016/j.powtec.2016.09.084.
[11] R. Censi, P. Di Martino, Polymorph impact on the bioavailability and stability of poorly soluble drugs, Molecules 20 (2015) 18759–18776, http://dx.doi.org/10.3390/molecules201018759.
[12] A. Tilborg, B. Norberg, J. Wouters, Pharmaceutical salts and cocrystals involving amino acids: a brief structural overview of the state-of-art, Eur. J. Med. Chem. 74 (2014) 411–426, http://dx.doi.org/10.1016/j.ejmech.2013.11.045.
[13] H. Grohganz, P.A. Priemel, K. Löbmann, L.H. Nielsen, R. Laitinen, A. Mullertz, G. Van den Mooter, T. Rades, Refining stability and dissolution rate of amorphous drug formulations, Expert Opin. Drug Deliv. 11 (2014) 977–989, http://dx.doi.org/10.1517/17425247.2014.911728.
[14] R. Laitinen, K. Löbmann, H. Grohganz, C. Strachan, T. Rades, Amino acids as Co-amorphous excipients for simvastatin and glibenclamide: physical properties and stability, Mol. Pharm. 11 (2014) 2381–2389, http://dx.doi.org/10.1021/mp500107s.
[15] V.B. Sterren, V. Aiassa, C. Garnero, Y.G. Linck, A.K. Chattah, G.A. Monti, M.R. Longhi, A. Zoppi, Preparation of Chloramphenicol/Amino acid combinations exhibiting enhanced dissolution rates and reduced drug-induced oxidative stress, AAPS PharmSciTech (2017), http://dx.doi.org/10.1208/s12249-017-0775-4.
[16] E. Lenz, K.T. Jensen, L.I. Blaabjerg, K. Knop, H. Grohganz, K. Löbmann, T. Rades, P. Kleinebudde, Solid-state properties and dissolution behaviour of tablets containing co-amorphous indomethacin-arginine, Eur. J. Pharm. Biopharm. 96 (2015) 44–52, http://dx.doi.org/10.1016/j.ejpb.2015.07.011.
[17] N. Kamei, E.-S. Khafagy, J. Hirose, M. Takeda-Morishita, Potential of single cationic amino acid molecule arginine for stimulating oral absorption of insulin, Int. J. Pharm. 521 (2017) 176–183, http://dx.doi.org/10.1016/j.ijpharm.2017.01.066.
[18] P. Jadhav, B. Petkar, Y. Pore, A. Kulkarni, K. Burade, Physicochemical and molecular modeling studies of cefixime–L-arginine–cyclodextrin ternary inclusion compounds, Carbohydr. Polym. 98 (2013) 1317–1325, http://dx.doi.org/10.1016/j.carbpol.2013.07.070.
[19] P.V.M. Vikmon, I. Kolbe, J. Szejtli, Preparation and characterization of piroxicam alkali-salt β-cyclodextrin complexes, proceed 9th intern symp cyclodextrins, dordrecht, Ger. Kluwer Acad. Publ. (1999) 281–284.
[20] E. Redenti, L. Szente, J. Szejtli, Cyclodextrin complexes of salts of acidic drugs, Thermodyn. Prop. Struct. Features Pharm. Appl. 90 (2001) 979–986.
[21] G. Piel, B. Pirotte, I. Delneuville, P. Neven, G. Llabres, J. Delarge, L. Delattre, Study of the influence of both cyclodextrins and L-lysine on the aqueous solubility of nimesulide; isolation and characterization of nimesulide-L –Lysine-cyclodextrin complexes, J. Pharm. Sci. 86 (1997) 475–480.
[22] P. Mura, F. Maestrelli, M. Cirri, Ternary systems of naproxen with hydroxypropyl-β-cyclodextrin and aminoacids, Int. J. Pharm. 260 (2003) 293–302, http://dx.doi.org/10.1016/S0378-5173(03)00265-5.
[23] P. Mura, G. Piero, M. Cirri, F. Maestrelli, M. Sorrenti, L. Catenacci, Solid-state characterization and dissolution properties of Naproxen –Arginine -Hydroxypropyl-β-cyclodextrin ternary system, Eur. J. Pharm. Biopharm. 59 (2005) 99–106, http://dx.doi.org/10.1016/j.ejpb.2004.05.005.
[24] A. Figueiras, J.M.G. Sarraguça, Pais A.A.C.C, R.A. Carvalho, J.F. Veiga, The role of l –arginine in inclusion complexes of omeprazole with cyclodextrins, AAPS PharmSciTech 11 (2010), http://dx.doi.org/10.1208/s12249-009-9375-2.
[25] FDA, Center for drug evaluation and research (CDER), in: The Biopharmaceutics Classification Systems (BCS) Guidance, Food and Drug Administration, U.S, 2001.
[26] L.H. Nielsen, T. Rades, A. Müllertz, Stabilisation of amorphous furosemide increases the oral drug bioavailability in rats, Int. J. Pharm. 490 (2015) 334–340, http://dx.doi.org/10.1016/j.ijpharm.2015.05.063.
[27] C. Garnero, A.K. Chattah, M. Longhi, Stability of furosemide polymorphs and the effects of complex formation with β-cyclodextrin and maltodextrin, Carbohydr. Polym. 152 (2016) 598–604, http://dx.doi.org/10.1016/j.carbpol.2016.07.006.
[28] A. Tilborg, B. Norberg, J. Wouters, Pharmaceutical salts and cocrystals involving amino acids: a brief structural overview of the state-of-art, Eur. J. Med. Chem. 74 (2014) 411–426, http://dx.doi.org/10.1016/j.ejmech.2013.11.045.
[29] C.S. Mangolim, C. Moriwaki, A.C. Nogueira, F. Sato, M.L. Baesso, A.M. Neto, G. Matioli, Curcumin-β-cyclodextrin inclusion complex: stability, solubility, characterisation by FT-IR, FT-Raman, X-ray diffraction and photoacoustic spectroscopy, and food application, Food Chem. 153 (2014) 361–370, http://dx.doi.org/10.1016/j.foodchem.2013.12.067.
[30] M. Lukasiewicz, S. Kowalski, A. Ptaszek, P. Ptaszek, β-Cyclodextrin as water-solubility enhancer for butylated hydroxytoluene, Chem. Pap. 69 (2015) 747–755, http://dx.doi.org/10.1515/chempap-2015-0078.
[31] M. Sousdaleff, M.L. Baesso, A.M. Neto, A.C. Nogueira, V.A. Marcolino, G. Matioli, Microencapsulation by freeze-drying of potassium norbixinate and curcumin with maltodextrin: stability, solubility, and food application, J. Agric. Food Chem. 61 (2013) 955–965, http://dx.doi.org/10.1021/jf304047g.
[32] T. Higuchi, K.A. Connors, Phase-Solubility techniques in advances in analytical chemistry and instrumentation, Intersci. New York 4 (1965) 117–212.
[33] W.J. Moore, H.H. Flanner, Mathematical comparison of dissolution profiles, Pharm. Technol. 20 (1996) 64–74.
[34] P. Costa, An alternative method to the evaluation of similarity factor in dissolution testing, Int. J. Pharm. 220 (2001) 77–83.
[35] C. Garnero, A.K. Chattah, M. Longhi, Supramolecular complexes of maltodextrin and furosemide polymorphs: a new approach for delivery systems, Carbohydr. Polym. 94 (2013) 292–300, http://dx.doi.org/10.1016/j.carbpol.2013.01.055.
[36] C. Garnero, A.K. Chattah, M. Longhi, Improving furosemide polymorphs properties through supramolecular complexes of β-cyclodextrin, J. Pharm. Biomed. Anal. 95 (2014) 139–145, http://dx.doi.org/10.1016/j.jpba.2014.02.017.
[37] K.T. Jensen, F.H. Larsen, K. Löbmann, T. Rades, H. Grohganz, Influence of variation in molar ratio on co-amorphous drug-amino acid systems, Eur. J. Pharm. Biopharm. 107 (2016) 32–39, http://dx.doi.org/10.1016/j.ejpb.2016.06.020.
[38] C. Doherty, P. York, Frusemide crystal forms; solids state and physicochemical analyses, Int. J. Pharm. 47 (1988) 141–155.
[39] T. Ueto, N. Takata, N. Muroyama, A. Nedu, A. Sasaki, S. Tanida, K. Terada, Polymorphs and a hydrate of furosemide-Nicotinamide 1: 1 cocrystal, Cryst. Growth Des. 12 (2012) 485–494.
[40] Y. Matsuda, E. Tatsumi, Physicochemical characterization of furosemide modifications, Int. J. Pharm. 60 (1990) 11–26, http://dx.doi.org/10.1016/0378-5173(90)90185-7.
[41] N.J. Babu, S. Cherukuvada, R. Thakuria, A. Nangia, Conformational and synthon polymorphism in furosemide (Lasix), Cryst. Growth Des. 10 (2010) 1979–1989, http://dx.doi.org/10.1021/cg100098z.